Investigation of the Impact of Connection Stiffness on random Vibration Testing

Liuyuan Tao

Yonghong Aviation Machinery Co., Ltd., Guiyang 550000, Guizhou Province, China
Corresponding author's e-mail: 493965816@qq.com

Abstract. This investigation aimed to examine the impact of connection stiffness on random vibration testing of heat sink products. The approach involved developing a finite element model of the test piece and fixture, and conducting simulated studies on random vibration testing under varying connection stiffness conditions, in conjunction with actual test results. The findings demonstrated that by adjusting the stiffness of the test piece and fixture models based on real test data, the calculated results closely aligned with experimental outcomes, effectively rectifying inaccuracies in finite element analysis. In summary, it was observed that different forms of connection led to diverse connection stiffness, which emerged as a primary factor influencing overall modal characteristics of both the test piece and fixture as well as significantly impacting simulation outcomes.

Keywords: connection stiffness,random vibration

1 Introduction

Finite Element Simulation Analysis: Enhancing Accuracy in Vibration Testing. Vibration testing using finite element simulation has become integral to the product development process due to its ability to identify potential defects early on while providing a foundation for subsequent measurements and monitoring activities. By establishing comprehensive finite element models incorporating dynamic calculation methods such as modal analysis, frequency response analysis, and random vibration analysis for both fixtures and test pieces (including the vibration table model where applicable), numerical simulations enable cost savings across testing equipment operation costs, product production costs, and human resources while expediting the research cycle.

Vibration test simulations have revealed discrepancies, leading to failures during actual tests. This highlights significant differences between simulated results and experimental outcomes. Our study identifies varying connection structures when designing test fixtures or selecting installation forms for impacting simulation results, a critical factor contributing to disparities between analytical predictions and experimental findings.

2 Foundational Theory

Random vibration analysis typically employs two methods [1]: time-domain analysis, which is based on statistical counting, and frequency-domain analysis, which relies on the power spectral density function. Frequency-domain analysis is commonly utilized [2], where the PSD function at critical points of the structure can be obtained through finite element modeling or testing. This information is then combined with the stress probability density function (PDF) to select appropriate cumulative damage criteria and failure criteria for estimating structural fatigue life.

The stress response PSD function can be calculated by inputting the load's PSD and the frequency response function (FRF) in practical engineering [3][4].

$$\mathrm{Sout}(\omega) = \mathrm{H}(\omega)2\mathrm{Sin}(\omega) \tag{1}$$

where Sout(ω) denotes the stress response PSD function; Sin(ω) denotes the known input PSD function.

The random vibration stress σ_{RMS} can be calculated by using the stress response PSD function as follows:

$$\sigma_{RMS} = \mathrm{Sout}(\omega)\mathrm{d}\omega \tag{2}$$

where H(ω) is the inherent characteristic of the structure, which reflects the amplitude and phase changes of the steady-state response of the mechanism under a harmonic external excitation.

$$\mathrm{H}_{\omega} = \mathrm{k} - \mathrm{m}\omega^2 + jc\omega \tag{3}$$

where K represents the structural stiffness; M represents the structural mass; C represents the damping.

From the above formula, it is evident that, given a known input load, the stress response is influenced by three factors: mass, stiffness, and damping. Structural modeling software currently provides relatively accurate estimations of mass; thus, the distribution of mass in the finite element model has minimal impact on the accuracy of analysis results. Consequently, only 2.5% of structural damping is typically considered during the analysis [5]. When the stiffness of the model structure closely aligns with that of the test piece's actual situation, random vibration analysis results will closely approximate test results. Therefore, a finite element model is established for different connection forms to calculate their modal values and compare them with experimental results to investigate how simulation models' representation of stiffness influences random vibration when structures adopt different connections. Furthermore, this study aims to analyze how connection stiffness affects random vibration.

3 Typical Forms of Connection

The manufacturing processes for trial fixtures include overall machining, casting, welding, bolt connection, and adhesion. Overall, machining is known for its high precision,

short cycle times, and excellent vibration transmission properties, making it suitable for the production of small trial fixtures. Casting can be used to fabricate intricate large fixtures with robust rigidity and damping characteristics. Welding is appropriate for fixtures with relatively simple structures and low cost. While bolted fixtures may have inferior dynamic characteristics, they are easy to install and disassemble. Adhesion is primarily utilized in the production of small fixtures but is generally not employed.

3.1 Monolithic Molded Structure

3.1.1 Structural and Finite Element Modeling. The monolithic molded structure is constructed from sheet metal and machining or additive manufacturing, which can be regarded as a monolithic material. As depicted in Figure 1, a partition is formed through sheet metal forming and stamping, utilizing 1Cr18Ni9Ti stainless steel as the material. It possesses a modulus of elasticity of 199 GPa and a density of 7.9 g/mm^3. Utilizing ANSYS for diaphragm modeling and modal analysis, the first two natural frequencies in the free state were determined to be 60.0 Hz and 159.2 Hz, as illustrated in Figure 2.

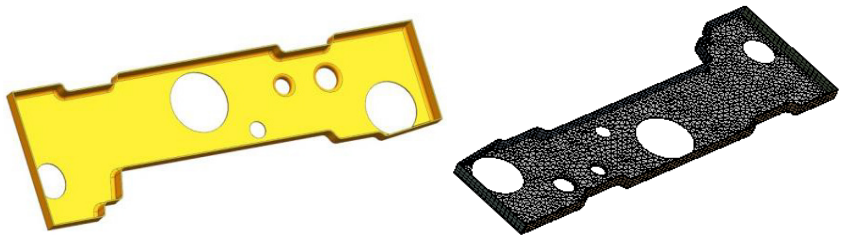

Fig. 1. Schematic of shear wall structure and its finite element model.

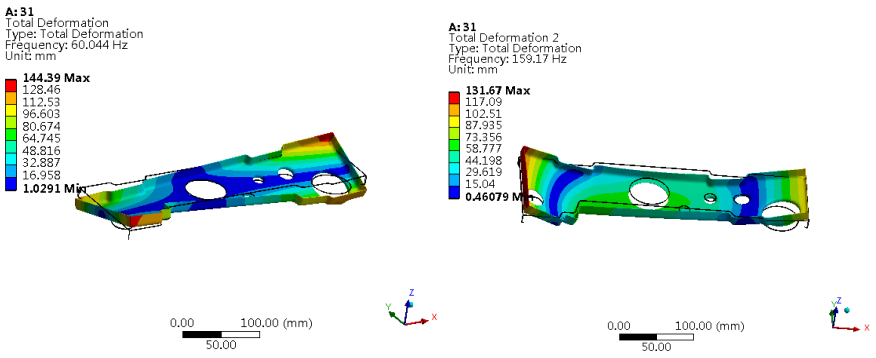

Fig. 2. The first two modalities of the shear wall structure.

3.1.2 Empirical Comparative Analysis. The modal frequencies of the diaphragm were determined through modal testing using an Impact Hammer, as depicted in Figure 3 and Figure 4. The obtained test results indicate frequencies of 55.63 Hz, 107.50 Hz, and 163.13 Hz, which are slightly higher than the calculated values at 107.50 Hz. This discrepancy may be attributed to the rigid support system. A comparison between finite element analysis and experimental results reveals errors of 9.1% and 2.5%, respectively, for the diaphragm's behavior. Despite these discrepancies, the calculated results align with the requirements for practical engineering applications, demonstrating higher accuracy in predicting overall structural behavior when isolated from other connections.

Fig. 3. Location of test measurement points.

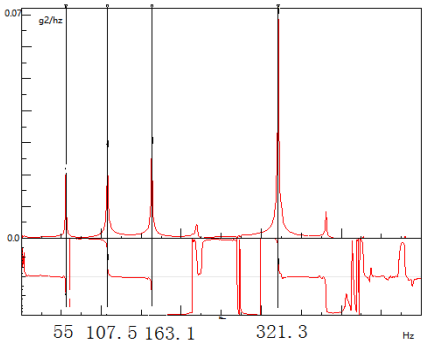

Fig. 4. Test findings.

3.2 Welded Structural Assembly

Welding, also referred to as joining engineering, involves the application of heat, pressure, or both to achieve an atomic-level bond between two parts. This results in a permanent connection not only at the macroscopic level but also at the microscopic level. It finds extensive applications in industrial sectors such as petrochemicals, power generation, and aerospace.

3.2.1 Structural and Finite Element Modeling. The structure depicted in Figure 5 is a fixture, and Figure 6 is finite element modeling. We predominantly utilize welding connections, which are fabricated from aluminum alloy with a modulus of elasticity of 71 GPa and a density of 2.7 g/mm^3. The finite element model employs the contact (Bonded) feature provided by ANSYS to simulate the welding connection between the two components. The modal analysis results for the fixture, derived from the calculations, are presented in Figures 7～10, showing the first four modal frequencies as 200.0 Hz, 350.8 Hz, 431.9 Hz, and 508.2 Hz.

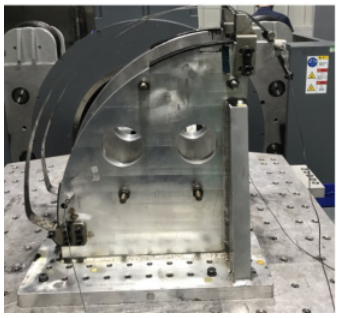

Fig. 5. Location of test measurement points.

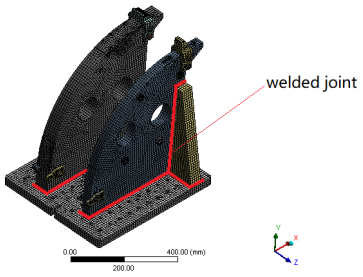

Fig. 6. Finite element modeling.

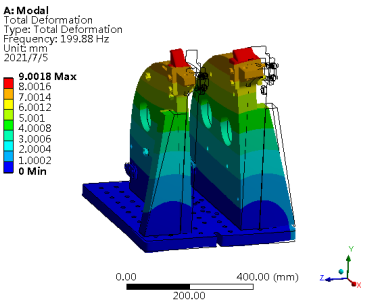

Fig. 7. 1st model.

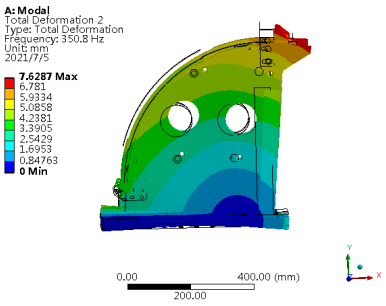

Fig. 8. 2nd model.

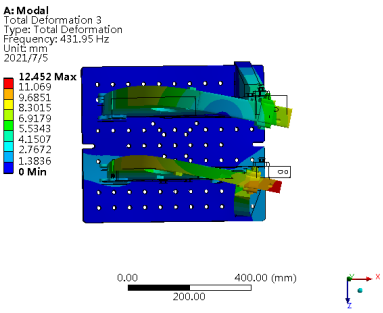

Fig. 9. 3rd model.

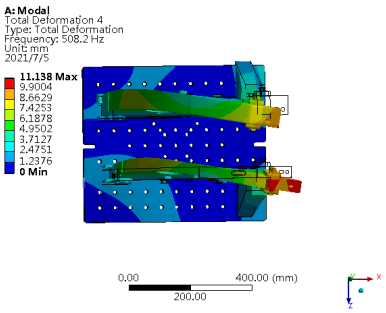

Fig. 10. 4th model.

Table 1. Computational and experimental error analysis of welded structural assembly.

Modal order	Computed value (Hz)	Measured value (Hz)	Error (%) [a]
1	200.0	210.5	5.0
2	350.8	325.0	-7.9
3	431.9	447.6	3.5

[a] $\text{Error} = (\text{Computed value} - \text{Measured value})/\text{Measured value} \times 100$

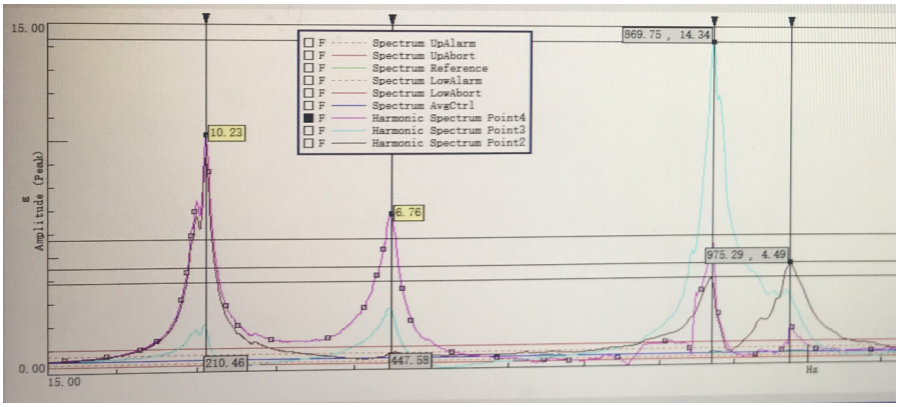

Fig. 11. Results of 1s[t] and 3[rd] frequency sweep experiment.

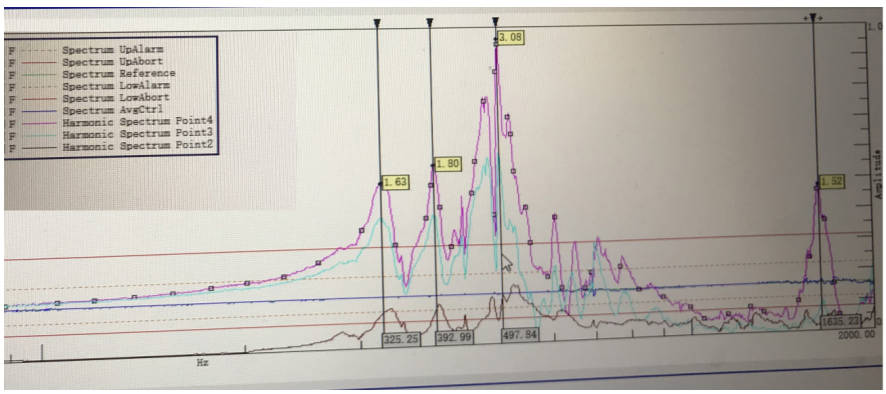

Fig. 12. Results of 2[nd] and 4[th] frequency sweep experiment.

3.2.2 Empirical Comparative Analysis. The data in Table 1 indicates the influence of welded joints on the inherent characteristics of the structure is investigated through experimental and analytical comparisons. Modal frequencies are determined by using a 0.5 g sinusoidal sweep method, with acceleration sensors strategically placed based on the structure's mode shape diagram, and the test results are depicted in Figures 11 and 12. The test results indicate that the welded connection permanently joins the two parts into a single entity, obviating the need for any special treatment when simulating the model.

3.3 Bolted connection Structure

Bolt connections often exhibit nonlinear connection stiffness due to clearance fit, posing challenges for finite element models in simulation. This paper presents the finite element simulation and experimental comparison of the elliptical hole bolt connection used in the test fixture design process.

3.3.1 Structural and Finite Element Modeling. The overall structure is depicted in Figures 13～14, with both the product and the fixture constructed from aluminum alloy featuring a modulus of elasticity of 71 GPa and a density of 2.8 g/mm^3. To facilitate test piece installation, elliptical holes were incorporated into the fixture structure, providing ample clearance and adjustable positioning. A finite element model was developed for the structure, with bolts and L support tightly fitting in the X and Y directions. The model employs the same contact method as welded connections, establishing the Z direction through frictional force between parts. Model 1 utilizes the first modeling method, assuming a non-sliding connection (6 degrees of freedom), while Model 2 adopts the second method, assuming no connection in the Z direction (remaining 5 degrees of freedom). Modal analysis for each model was separately conducted, with results presented in Figures 15～20.

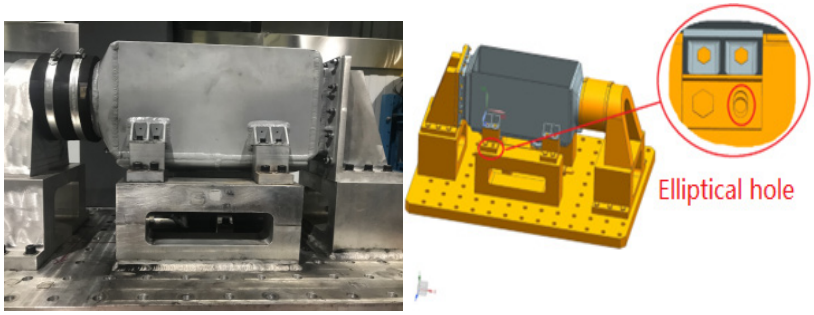

Fig. 13. Elliptical hole bolt connection structure.

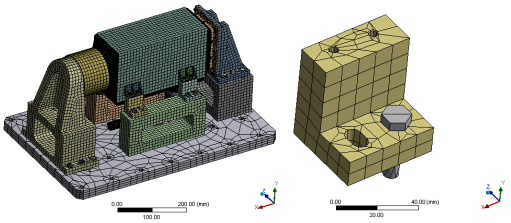

Fig. 14. Finite element modeling.

The modal analysis results of the two-state model indicate that, when connected, the frequencies of the six degrees of freedom are 497.6 Hz, 550.8 Hz, 693.9 Hz, and 757.9 Hz. Upon releasing the Z-axis connection, the first mode remains almost unchanged at 489.7 Hz, while the second mode decreases to 359.9 Hz, the third mode becomes 585.8 Hz, and the fourth mode is measured at 696.0 Hz.

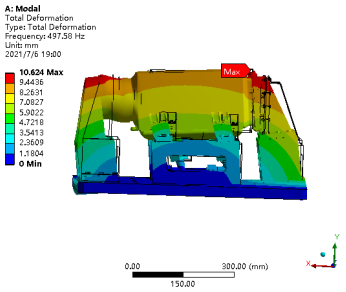

Fig. 15. 1st model of Mode 1.

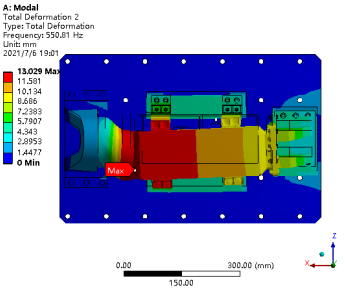

Fig. 16. 2nd model of Mode 1.

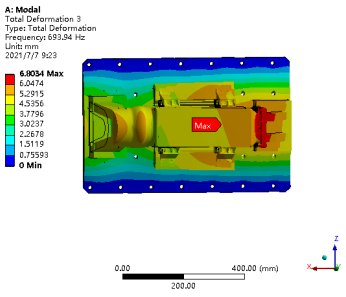

Fig. 17. 3rd model of Mode 1.

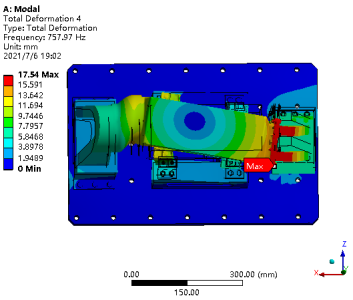

Fig. 18. 4th model of Mode 1.

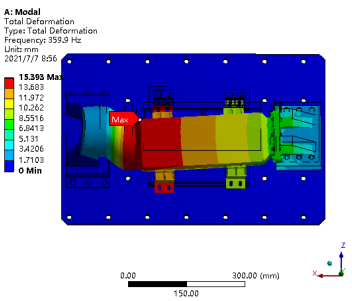

Fig. 19. 5th model of Mode 1.

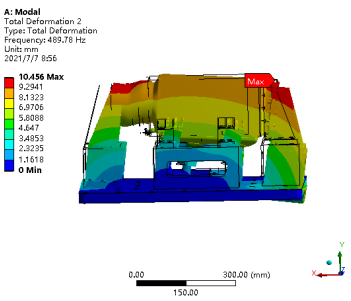

Fig. 20. 6th model of Mode 1.

3.3.2 Empirical Comparative Analysis. Through experimental and comparative analysis, the study investigates the impact of bolt gaps on the structural inherent characteristics and validates the effectiveness of two modeling methods. The structure's modal frequencies are examined by using a 0.5 g sinusoidal sweep method, with acceleration sensors strategically placed based on the structure's mode shape diagram, as depicted in Figures 16 and 17.

Table 2. Computational and experimental error analysis of bolted connection structure.

Modal order	Model 1 computed value (Hz)	Model 2 computed value (Hz)	Measured value (Hz)	Error1 (%) [a]	Error2 (%) [b]
1	497.6	359.9	345.2	-44.1%	-4.3%
2	550.8	489.7	473.2	-16.4%	-3.5%
3	693.9	585.8	543.6	-27.6%	-7.8%
4	757.9	696.0	789.3	4.0%	11.8%
5	497.6	359.9	345.2	-44.1%	-4.3%
6	550.8	489.7	473.2	-16.4%	-3.5%

[a] $\text{Error1} = (\text{Model 1 computed value} - \text{Measured value}) / \text{Measured value} \times 100$

[b] $\text{Error2} = (\text{Model 2 computed value} - \text{Measured value}) / \text{Measured value} \times 100$

The test results are presented in Figure 21 ~ Figure 24, indicating modal frequencies of 345.2 Hz, 473.2 Hz, 543.6 Hz, and 789.3 Hz. A comparison between the test results and the analysis findings is detailed in Table 2, revealing a significantly larger error for Model 1 than for Model 2. This suggests that the connection stiffness provided by friction force in the gap bolt connection direction may be disregarded; hence, modifications to the model based on test results are necessary to achieve more accurate calculation outcomes [6].

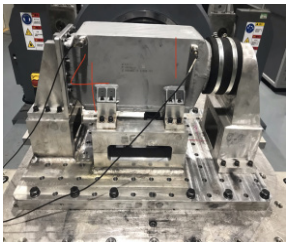

Fig. 21. Validation of the sensor placements for the 2nd and 4th models.

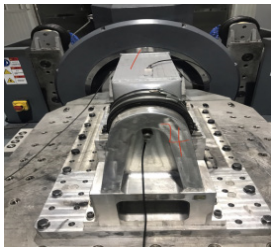

Fig. 22. Validation of the sensor placements for the 1st and 3rd models.

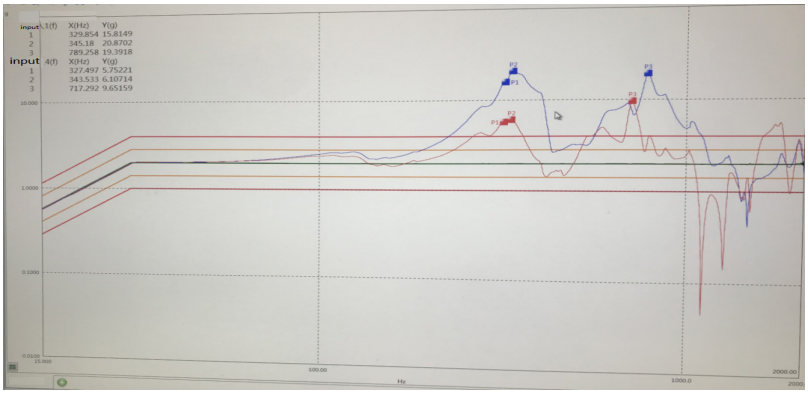

Fig. 23. Results of 1st and 3rd frequency sweep experiment.

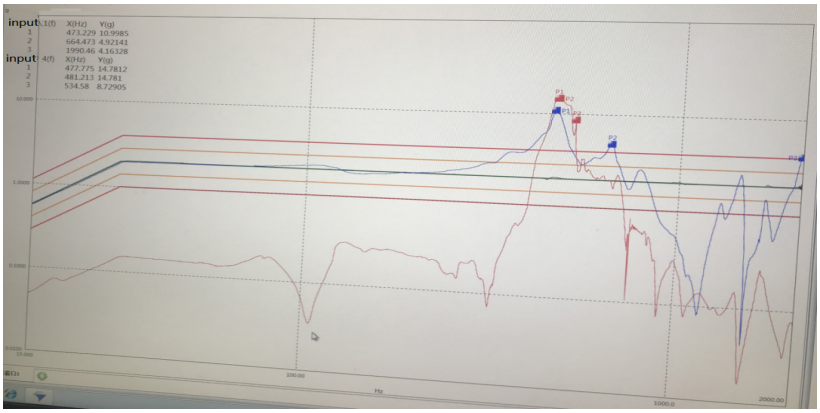

Fig. 24. Results of 2nd and 4th frequency sweep experiment.

4 An Investigation Into the Impacts of Random Vibration Testing

In Section 3.3, the structure contains two pipe fittings that require pressurization during random vibration testing. As a result, two L-shaped caps (in Figure 25) were installed and secured using clamps. The axial movement of the caps was constrained by the frictional force between the clamps and the caps.

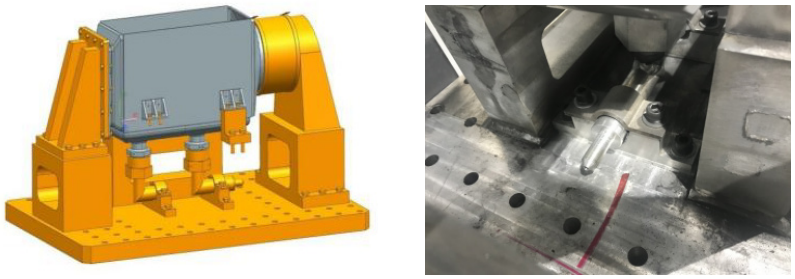

Fig. 25. Schematic of pipe cap and plug.

The product is constructed from 6061 aluminum alloy, and its mechanical properties are detailed in Table 3 of the "China Materials Engineering Canon".

Table 3. Properties of materials.

Grade of material	Density g/cm^3	Modulus of elasticity (GPa)	Poisson's ratio	Yield strength (MPa)	Tensile strength (MPa)	Fatigue limit (MPa)
6061	2.7	72	0.33	262	310	97

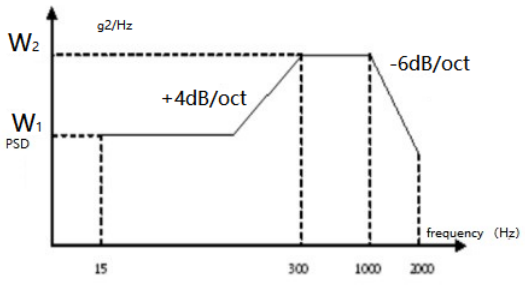

Fig. 26. Vibration test power spectrum.

In accordance with the specified requirements, the product will undergo endurance vibration tests as per GJB150.16A-2009, Methods for Environmental Testing of Military Equipment, Part 16: Vibration Test. The product will be subjected to 30 hours of endurance testing in each axis (X, Y, and Z), and it must demonstrate no signs of damage or impairment that would affect its functionality. The input load for the test is Sin(ω), as depicted in Figure 26.

4.1 The Initial Phase of Computational Analysis

It is assumed that full clamping of the L-shaped plug provides radial and axial restraint as well as free lateral rotation, as depicted in Figure 27. Under these connection stiffness conditions and assuming a structural damping factor of 2.5%, the results of random vibration analysis for the product are illustrated in Figures 28 to 30.

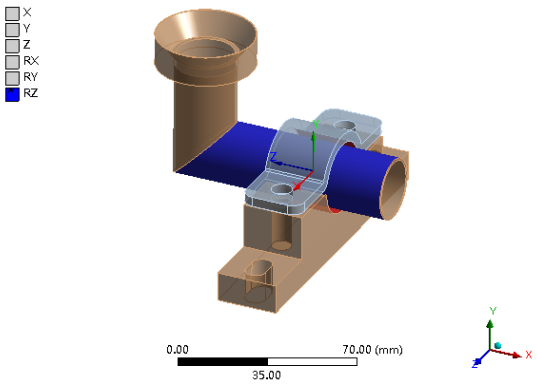

Fig. 27. L-shaped plug connection with a single degree of freedom, specifically azimuthal RZ freedom only.

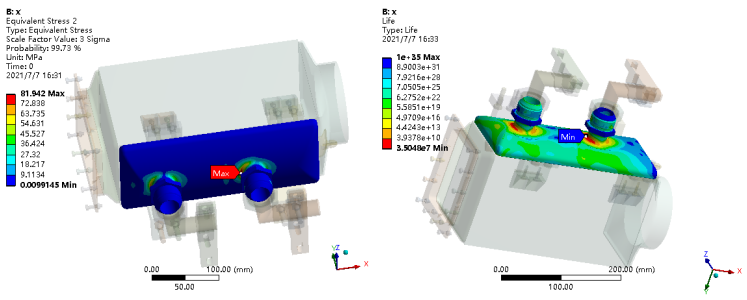

Fig. 28. X-axis random vibration 3σ RMS stress and life cloud char.

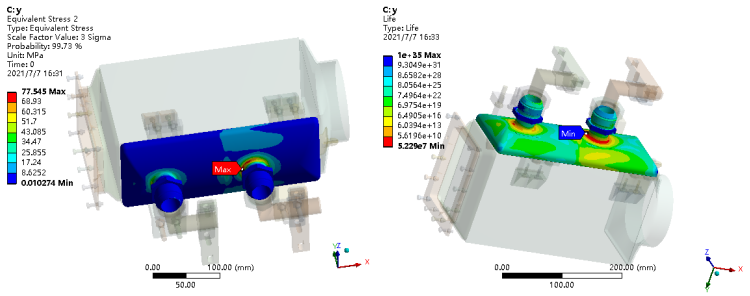

Fig. 29. Y-axis random vibration 3σ RMS stress and life cloud char.

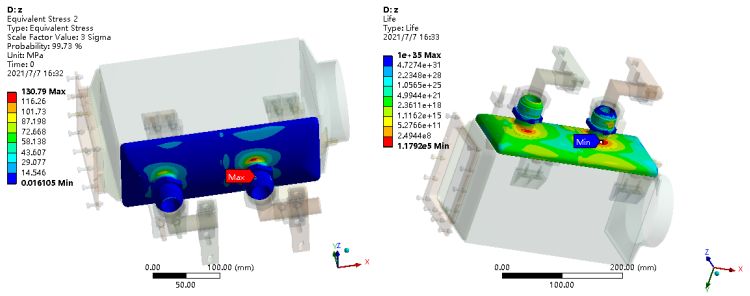

Fig. 30. Z-axis random vibration 3σ RMS stress and life cloud char.

The operational lifespan of the nozzle tip in three directions is as follows: X-axis – 9, 735.6 hours (35, 048, 000 seconds), Y-axis – 14, 525.0 hours (522, 900 seconds). The total damage calculation for the three-axis 90h test considering damage accumulation is as follows [7] [8]:

$$D = D_x + D_y + D_z \tag{4}$$

where D denotes the total damage; D_x denotes the X-axis damage; D_y denotes the Y-axis damage; D_z denotes the Z-axis damage.

Given that the total damage D is calculated as 30 x 19, 735.6 + 30 x 11, 452.5 + 30 x 132.8 = 0.921, and it is less than 1, the requirement of withstanding testing in all directions for 30 hours without being destroyed is satisfied. The analysis indicates that the structural fatigue life meets the specified criteria. However, despite only undergoing a two-hour test, the nozzle detached (in Figure 31). Discrepancies between finite element calculations and actual test results reveal a significantly shorter actual lifespan compared to the calculated one.

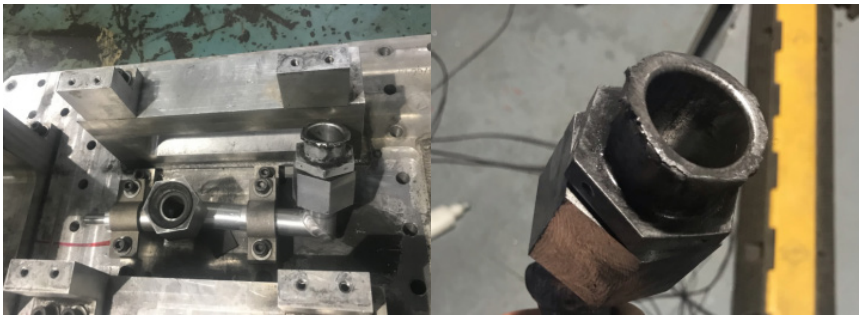

Fig. 31. Product test failure diagram.

4.2 The Subsequent Computational Analysis

When considering the axial connection stiffness of the L-shaped plug, it is prudent to release the Z-axis degree of freedom conservatively during estimation, as there may be a slightly lower stiffness in practice (which can be simulated by spring elements). The results of random vibration analysis for the product are illustrated in Figures 32～35.

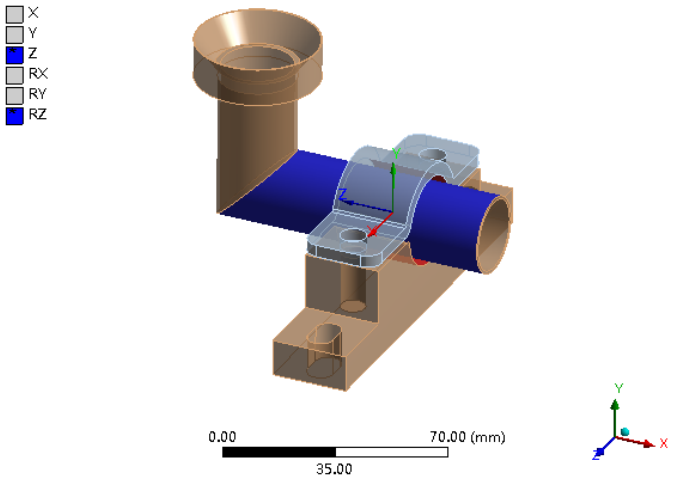

Fig. 32. L-shaped plug connection with a single degree of freedom, specifically azimuthal RZ freedom only.

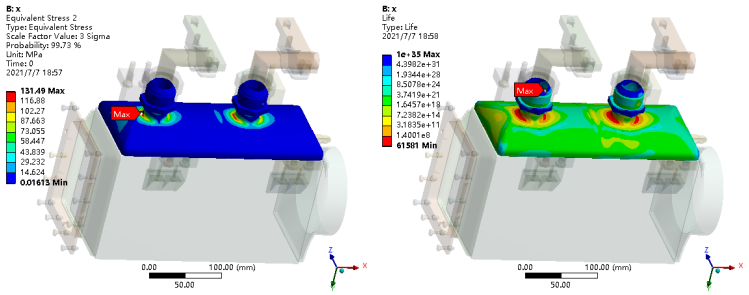

Fig. 33. X-axis random vibration 3σ RMS stress and life cloud char.

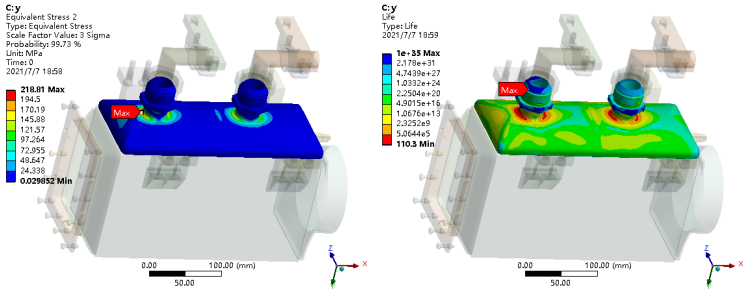

Fig. 34. Y-axis random vibration 3σ RMS stress and life cloud char.

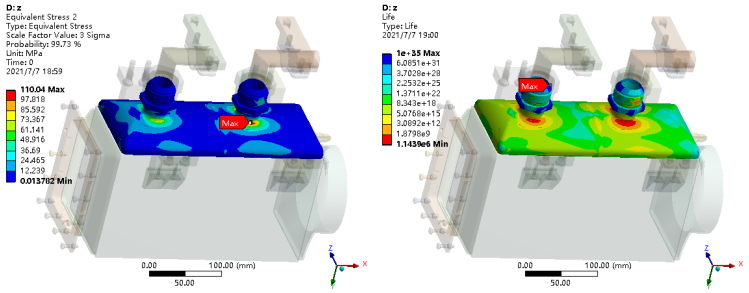

Fig. 35. Z-axis random vibration 3σ RMS stress and life cloud char.

The fatigue life of the nozzle tip in three directions is as follows: X direction - 17.1 hours (61, 581 seconds), Y direction - 0.03 hours (110.3 seconds), and Z direction - 317.8 hours (1, 143, 900 seconds). The calculation results show that the product only meets the 30-hour durability test requirement in the Z direction, while the X and Y directions do not meet the requirement, and the Y direction will be destroyed quickly, requiring either strengthening of the product itself or improvement of the fixture.

The fixture structure was enhanced based on the aforementioned analysis to align with the actual product installation form, leading to the successful completion of the testing process.

5 Conclusion

Based on experimental and simulation research presented in this paper, we draw several key conclusions:

- The stiffness of connections between whole parts and welded components are equivalent, allowing for their treatment as an integrated unit within finite element modeling.
- Adjustments are necessary for local stiffness at gaps in bolt connections with substantial clearances.
- Connection stiffness significantly influences simulation outcomes and should therefore take precedence during vibration test design.

References

1. Jiang Huiqiang. LSTM-Based Dynamic Response Prediction Method and Vibration Fatigue Life Analysis for Aerospace Structures [D]. Nanchang, Jiangxi: Nanchang University, 2023.
2. SUN Yue, LIU Xiaofeng, and SUN Wei. Vibration analysis of a hard-coating thin plate under random excitation using FEM and estimation of vibration reduction effect [J]. Journal of Vibration and Shock, 2022, 41 (4), 63-69.
3. Zuo P., Shi X. J., Ge R. W., et al. Unified series solution for thermal vibration analysis of composite laminated joined conical-cylindrical shell with general boundary conditions [J]. Thin-Walled Structures, 2022, 178: 109, 525.
4. Liu Fen, Wang Jianming, and Li Xiaoxiao. Research on Random Vibration Fatigue Life of Water Tank Welds in Motor Trains Using Time-Domain Method [J]. Materials Protection, 2020, 53 (8): 63-67.
5. Zhu Yuanfu. Simulation of system-level product vibration testing. Strength and Environment, 2003, 11 (4): 59-62.
6. Li Dong. Reduction and Correction of Finite Element Model for Aero-Engine Rotor Dynamics [D]. Beijing: Beijing University of Chemical Technology, 2022.
7. Aodi Yu. Fatigue Life Prediction and Reliability Analysis of Aero-engine Main Bearings [D]. Sichuan: University of Electronic Science and Technology of China, 2022.
8. Daiyang Gao. Frequency Domain Method for Multiaxial Vibration Fatigue Life Prediction of Structures [D]. Nanjing University of Aeronautics and Astronautics, 2020.